

# CrystEngComm

Accepted Manuscript



This is an *Accepted Manuscript*, which has been through the Royal Society of Chemistry peer review process and has been accepted for publication.

*Accepted Manuscripts* are published online shortly after acceptance, before technical editing, formatting and proof reading. Using this free service, authors can make their results available to the community, in citable form, before we publish the edited article. We will replace this *Accepted Manuscript* with the edited and formatted *Advance Article* as soon as it is available.

You can find more information about *Accepted Manuscripts* in the [Information for Authors](#).

Please note that technical editing may introduce minor changes to the text and/or graphics, which may alter content. The journal's standard [Terms & Conditions](#) and the [Ethical guidelines](#) still apply. In no event shall the Royal Society of Chemistry be held responsible for any errors or omissions in this *Accepted Manuscript* or any consequences arising from the use of any information it contains.

## ARTICLE

## Tuning the radial structure of core-shell silicon carbide nanowires

Cite this: DOI: 10.1039/x0xx00000x

M. Negri<sup>ab</sup>, S. C. Dhanabalan<sup>b</sup>, G. Attolini<sup>b</sup>, P. Lagonegro<sup>ab</sup>, M. Campanini<sup>ab</sup>, M. Bosi<sup>b</sup>, F. Fabbri<sup>b</sup> and G. Salviati<sup>b</sup>

Received 00th January 2012,  
Accepted 00th January 2012

DOI: 10.1039/x0xx00000x

[www.rsc.org/](http://www.rsc.org/)

The influence of growth condition over structural properties is reported for core-shell SiC/SiO<sub>2</sub> nanowires grown on silicon substrates by Chemical vapour deposition (CVD) technique.

Scanning Electron Microscope (SEM) and Transmission Electron Microscope (TEM) studies show a correlation between the growth temperature and nanowires structure and highlight the possibility to control the inner core diameter varying precursor concentration.

The nanowires covering of the substrate was considerably enhanced and homogenized using drop casting surfactant-aided deposition of catalyst on H-terminated silicon 100 surface.

### Introduction

One of the most important issues in nanoscience is to reach well-known and well-controlled growth techniques in order to obtain reliable structures for nanoelectronics, nanophotonics and biomedical applications<sup>1</sup>.

Self-assembly processes are promising to obtain novel heterostructures at the nano-scale acting as building blocks in such systems even though the understanding and the control over this kind of processes still have to be refined.

We recently demonstrated the possibility to obtain a selective growth of core-shell silicon carbide silicon oxide nanowires on a patterned silicon substrate<sup>2</sup>.

Cubic silicon carbide (3C-SiC or  $\beta$ -SiC) is a wide band gap semiconductor widely studied for its well-known properties such as its high temperature stability, thermal conductivity, hardness, chemical stability<sup>3</sup> and its biocompatibility<sup>4-6</sup> makes of SiC an optimum choice for devices to be implanted in biological systems.

Many efforts have been devoted in developing various synthesis methods to obtain SiC nanowires: CVD technique<sup>7</sup> or direct reactions such as carbothermal reduction of silica<sup>8</sup> or catalyst-assisted polymeric precursor pyrolysis method<sup>9</sup> are the most exploited, but also physical vapour transport (PVT)<sup>10</sup>, laser ablation<sup>11</sup>, arc discharge<sup>12</sup>, growth from solution<sup>13</sup> or carbon nanotube template-mediated growth (also called carbon nanotube-confined reaction method)<sup>14</sup> have been used.

Complex processes and manipulation are involved in many of these synthetic approaches, while the advantages of the CVD technique are its low cost, the possibility of high growth rates on large areas and the control of the shape and composition of nanostructures by changing the growth parameters.

Core-shell SiC/SiO<sub>2</sub> self-assembled nanostructures take advantage of the different materials properties: SiC nanowires have excellent elasticity and strength, higher than that of bulk SiC<sup>15</sup> while the silicon oxide shell can be easily functionalized

in order to develop nano bio-sensors<sup>16</sup> and both silicon carbide and silicon oxide are biocompatible materials.

Moreover we recently demonstrated the 3C-SiC emission enhancement in these nanowires due to the injection of carriers from the larger band-gap shell to the narrower band-gap core<sup>17</sup> with the possibility of tuning the light emission changing the core-to-shell ratio<sup>18</sup>.

In the present work we report on the variation of the self-assembled 3C-SiC core-shell nanowires radial structure changing the synthesis parameters, in particular the nanowires were synthesized at different temperatures and precursor concentrations with different catalysts to demonstrate the possibility to achieve a better control over shape and presence of the core.

In addition we developed a technique to obtain a uniform nanowires spatial density on silicon substrate by varying the catalyst solution composition.

Many studies highlighted nickel stimulation of neoplastic transformation<sup>19</sup>, consequently, in addition to the more commonly used nickel, iron catalyst was studied because it is more suitable for biomedical applications. The growth conditions comparison between iron nitrate and nickel nitrate catalysed nanowires (From here FecatNWs and NicatNWs) was carried out in order to verify the effect of different catalyst.

### Experimental

The nanowires synthesis was performed in a CVD reactor on Si (100) substrate with carbon monoxide (CO) as gaseous precursor. Nickel nitrate (Ni(NO<sub>3</sub>)<sub>2</sub>) and ferric nitrate (Fe(NO<sub>3</sub>)<sub>3</sub>) were used as catalysts.

Instead of utilizing a solid mixture of WO<sub>3</sub> and C as CO source, as previously proposed by Park et al.<sup>20</sup>, gaseous CO was used, allowing to obtain the control of precursor flow and concentration over time. Moreover this makes it possible to start the synthesis at the desired temperature, while, using the

solid precursor, the CO would be released at a fixed temperature<sup>21</sup>.

The catalysts were dissolved in ethanol and a non-ionic surfactant (oleylamine - O7805 Aldrich) was added to enhance ethanol wetting of silicon.

Substrates were previously cleaned with ultrasonic bath in organic solvent, etched in a hydrofluoric acid (HF) aqueous solution for 120 s to remove silicon oxide, rinsed in deionized water, dried in nitrogen atmosphere, dipped in catalyst solution and then dried at 40° C in air.

Substrates were positioned in the CVD system growth chamber which was then purged with N<sub>2</sub> to remove oxygen. Once reaching the growth temperature, after a short time for stabilization, CO was introduced for 15 minutes. Finally the growth chamber was cooled down to room temperature in nitrogen atmosphere.

The morphological characterization was carried out by Field Emission Gun Scanning Electron Microscope (FEG-SEM) (Jeol - 6400F). Radial structure was studied using Transmission Electron Microscope (TEM) (Jeol - JEM 2200 FS) for High-Resolution (HR-TEM) studies, High Angle Annular Dark Field imaging in Scanning mode (HAADF-STEM) and Energy Dispersive X-ray (EDX).

## Results and discussion

Silicon wafer HF treatment is a very well-known technique to remove silicon surface oxide and to obtain a stable H-terminated surface. The result of this process is a (100) Si surface with most of Si atoms bonded with 2 hydrogen atoms each (Figure 1) and small percentage of them bonded with 1 or 3 hydrogen atoms or oxygen or fluorine depending on the conditions of etching treatment (HF concentration, time, temperature, pH).

Water rinse after this treatment tends to remove fluorine terminations and to replace them with hydroxyl groups<sup>22</sup>.

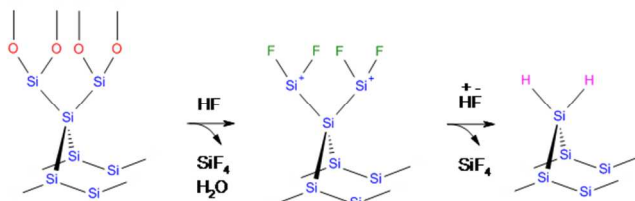


**Figure 1:** The possible mechanism of Si-H bond formation on Si (100) surface by HF-etching treatment (after Ubara et al.<sup>23</sup>).

The H-terminated silicon surface is hydrophobic, and the wettability is limited for water and ethanol. Following the classical Young equation for the contact angle of a liquid droplet on a solid surface<sup>24</sup>,  $\gamma_{sv} = \gamma_{sl} + \gamma_{lv} \cos\theta$  (where  $\gamma_{sv}$ ,  $\gamma_{sl}$  and  $\gamma_{lv}$  are, respectively, the surface tension between the solid and the vapour, the solid and the liquid and the liquid and the vapour, while  $\theta$  is the contact angle), the reduction of the contact angle can be achieved either decreasing  $\gamma_{lv}$  and  $\gamma_{sl}$  or increasing  $\gamma_{sv}$ , which means, in other words, a reduction of the total excess free energy<sup>25</sup>. We chose to reduce the ethanol solution surface tension by adding a non-ionic surfactant: oleylamine was added to catalyst ethanol solution, leading to the formation of a uniform film on silicon substrate after catalyst solution drop casting on silicon substrate. The liquid solution is easily dispersed onto the silicon surface thanks to the surfactant laying between the hydrophobic surface and the polar

liquid. A schematic view of surfactant distribution on H-terminated 100 Si surface is shown in Figure 2.

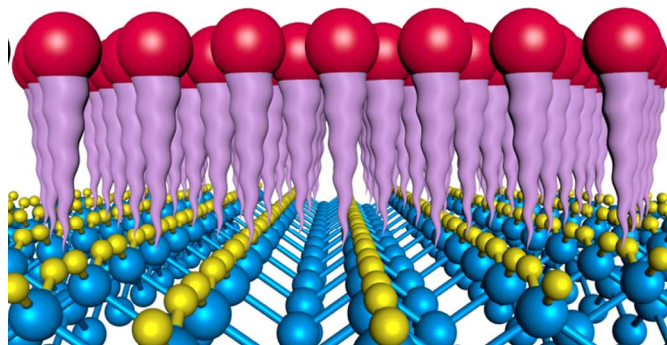


**Figure 2:** simplified view of surfactant distribution on H-terminated silicon 100 surface: each surface silicon atom (bigger spheres on the bottom of the image) is bonded to two hydrogen atoms (smaller spheres on the bottom). The hydrophobic part of oleylamine molecule (curvy tails of the molecules in the center of the image, in violet) is close to the silicon surface, while hydrophilic part (red spheres in the upper part of the image) is in contact with the polar ethanol solution (not shown in the image).

Thanks to the presence of the surfactant, even during the drying process, when ethanol evaporates and the catalyst concentration increases, the wetting of the substrate remains complete until a film of dry nitrate is formed on the silicon.

Both Ni(NO<sub>3</sub>)<sub>2</sub> and Fe(NO<sub>3</sub>)<sub>3</sub> undergo a decomposition during heating phase: nickel(II) nitrate decomposes to nickel(II) oxide and iron(III) nitrate to iron(III) oxide<sup>26</sup>, subsequently the dewetting process takes place and the catalyst forms droplets or “islands” on the substrate surface, in the same way as it happens in conventional vapour liquid solid (VLS) growth<sup>27</sup>.

A uniform catalyst distribution allows to obtain substrates fully covered with core-shell SiC/SiO<sub>2</sub> nanowires after the synthesis. A comparison between different nanowires samples is shown in Figure 3 (a) and (b).

The sample in Figure 3a was prepared using a solution of Ni(NO<sub>3</sub>)<sub>2</sub> in ethanol and simply depositing it on the silicon substrate. The result is the formation of some areas on its surface where there is higher nanowires spatial density (white stains). On the contrary the sample in Figure 3b was synthesized using the same catalyst solution added with oleylamine surfactant: the whole surface has a uniform grey colour because there is a constant nanowires spatial distribution. The growth conditions were: catalyst: Ni(NO<sub>3</sub>)<sub>2</sub> growth temperature: 1100° C, [CO] = 4% for a growth time of 15 minutes. Similar results were obtained with Fe(NO<sub>3</sub>)<sub>3</sub> as catalyst.

Areas covered with high density nanowires bundles are easily recognizable even with naked eye observation: the colour of the substrate is white or light grey. SEM images of the two samples are reported in fig. S1 in supplementary information.

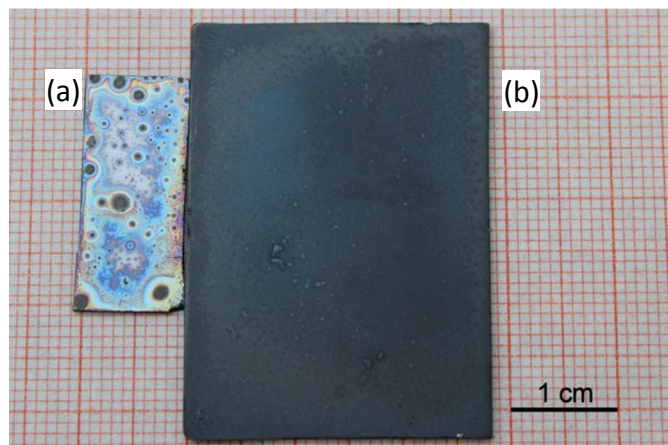


**Figure 3:** (a) silicon substrate covered by core shell SiC/SiO<sub>2</sub> nanowires (white areas) with catalyst deposition without using surfactant. (b) sample with core shell SiC/SiO<sub>2</sub> nanowires grown after catalyst deposition using oleylamine surfactant.

Figure 4 reports the size distribution of the NWs grown with different catalyst: the length for both samples is tens of microns, while the diameter for FecatNWs is slightly greater.

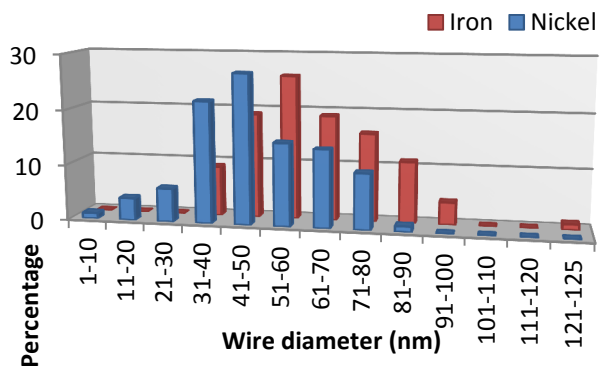


**Figure 4:** Wire diameters distribution for a sampling frame of 100 elements: the average is 49 nm for NicatNWs and 68 nm for FecatNWs

There isn't any evidence of morphological differences between the two sets of samples (FecatNWs and NicatNWs), nanowires form uniform bundles on all substrate as it can be seen in Figure 5a and it is possible to assess the presence of the catalyst on the nanowire tip suggesting a growth mechanism comparable to VLS. From SEM backscattered electrons observation and Transmission Electron Microscopy High-Angle Annular Dark-Field imaging (TEM-HAADF) (fig. S2 in supplementary information) it is possible to assess the presence of high-Z elements in the tip.

From TEM studies (Figure 5b), the nanowires are shown to exhibit a core-shell structure with an average core diameter of 20 nm. The core is 3C-SiC univocally identified by the crystal symmetry and the lattice spacings, the orientation is  $\langle 111 \rangle$  axis along the growth direction and we observed the occasional occurrence of stacking faults along (111) planes (Figure 5c).

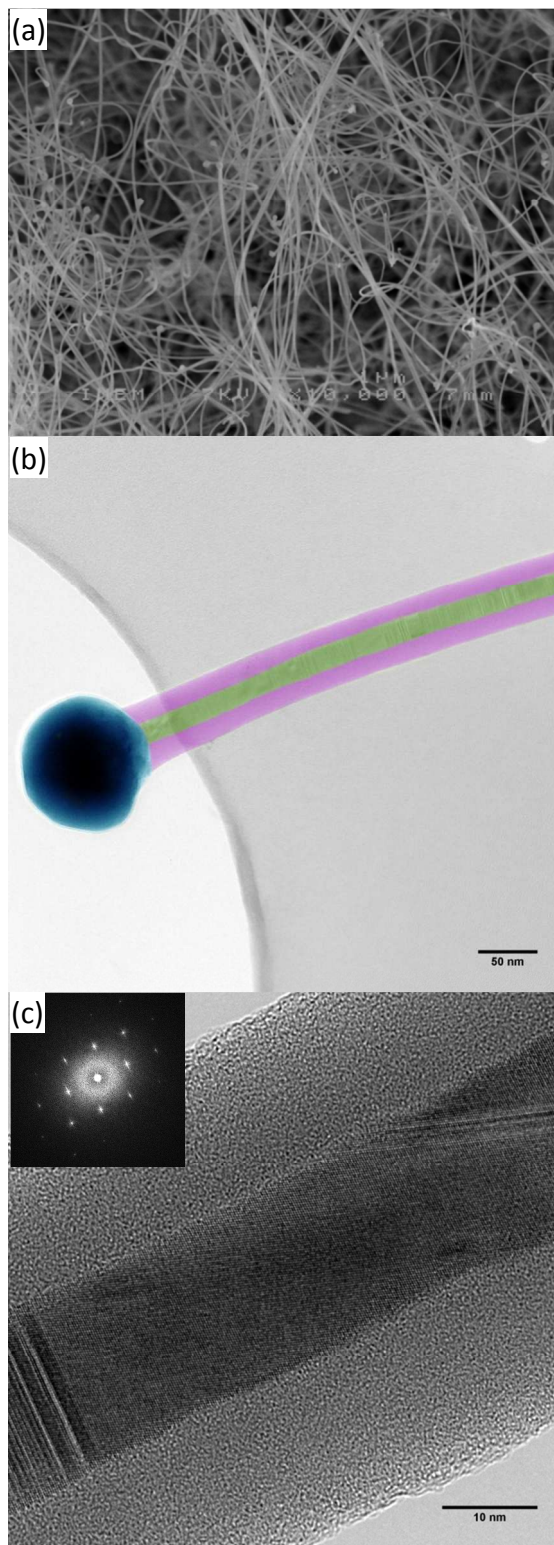


**Figure 5:** (a) Top view SEM image of a typical iron nitrate catalysed nanowires sample. (b) TEM false coloured image of a nanowire. The SiC core is highlighted in green, the SiO<sub>2</sub> shell is violet, while the catalyst tip is blue. (c) TEM high resolution detail of the wire: the crystalline order in the 3C-SiC core is clearly visible. In the lower-left part some stacking faults in the core SiC structure are evident as darker and lighter lines. In the inset the fast Fourier transform of the image.

The NW tip is crystalline, as verified by High Resolution TEM studies (Figure 6 a), and it contains the metal catalyst (Ni or Fe) alloyed with silicon (see a representative TEM-EDX spectrum reported in Figure 6b to form silicides or sometimes silicates, with traces of carbon.

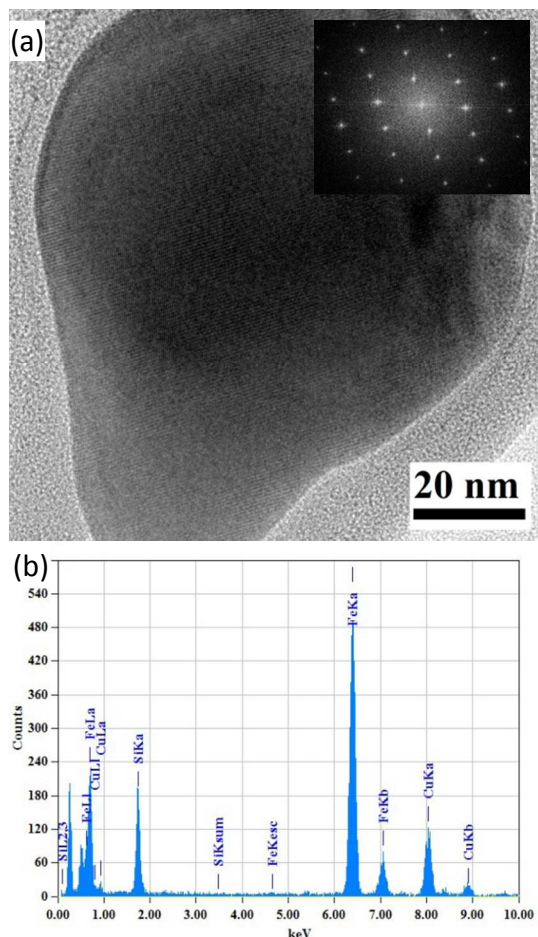


**Figure 6** a) High resolution TEM image of a single NW tip of the iron nitrate catalysed sample. The corresponding Fast Fourier Transform is shown as inset. (b) EDX spectrum acquired in spot mode on the NW tip. Silicon and iron peaks are detected (and Copper from TEM grid).

The effect of growth temperature on morphological and structural properties was investigated varying from 1050°C to 1150°C. The results are presented in Figure 7 and summarized in Table 1. With lower temperature (1050°C) in NicatNWs samples it was possible to observe NWs of pure  $\text{SiO}_x$  (with  $1 < x < 2$ )<sup>28</sup> without any SiC core. In the case of FecatNWs the growth does not occur, but it's possible to observe the catalyst dewetting (see fig. S3 in supplementary information). TEM images of samples synthesized at  $T=1070^\circ$  are shown in Figure 7 (a) and (b): nickel catalysed NWs have core-shell structure and some silicon oxide only, meanwhile FecatNWs are all  $\text{SiO}_x$  nanowires. We obtained regular core-shell structure for both NicatNWs and FecatNWs synthesized at 1100°C as pointed out in Figure 5. The results of the synthesis carried out at 1150°C are shown in Figure 7 (c) and (d): TEM observation reveals the growth of  $\text{SiO}_x$  NWs without the core-shell structure.

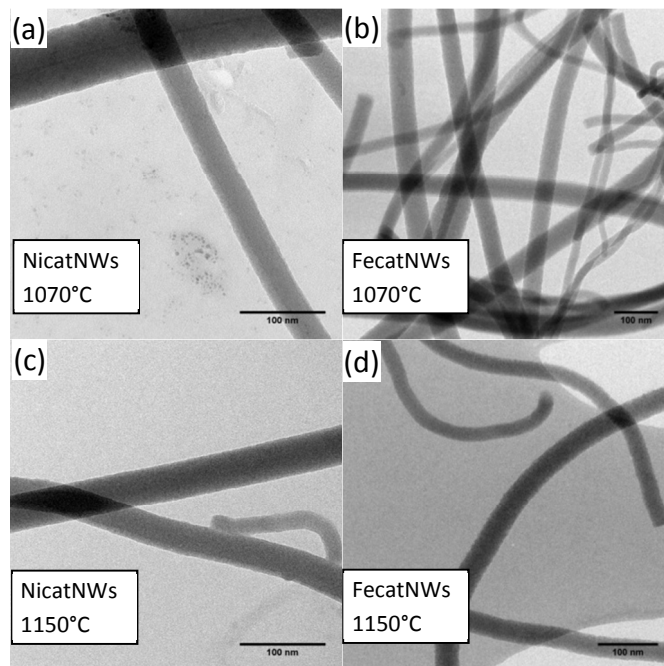


**Figure 7:** Temperature effect on core formation for  $\text{Ni}(\text{NO}_3)_2$  and  $\text{Fe}(\text{NO}_3)_3$  catalysed nanowires

**Table 1:** synthesis result for different growth temperatures and different catalysts

Synthesis T (°C)	$\text{Ni}(\text{NO}_3)_2$ catalysed NWs structure	$\text{Fe}(\text{NO}_3)_3$ catalysed NWs structure
1050	Amorphous	No growth
1070	Core/shell + Amorphous	Amorphous
1100	Core/shell	Core/shell
1150	Amorphous	Amorphous

Introducing gaseous CO in the system instead of using solid state precursors allows a precise tuning of precursor concentration over time. The effect of different CO concentration on the NWs radial structure was studied. As a reference a concentration of 4‰ was chosen. For all of these experiments the growth temperature was 1100°C, to guarantee the core-shell structure (see Table 1).

With lower concentration (2‰) (Figure 8 (a)) there was a significant reduction of core diameter in all the wires with respect to standard conditions (4‰), while increasing the CO concentration (16‰) (Figure 8 (b)) didn't lead to any significant morphological and structural change.

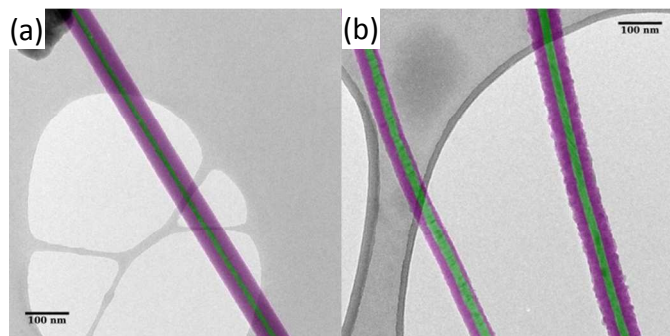


**Figure 8:** Images in false colours: the SiC core is highlighted in green and the SiO<sub>2</sub> shell is violet. (a) STEM-HAADF image of a sample synthesized at lower precursor concentration. (b) TEM image of two wires in a sample synthesized at higher CO concentration. In dark-field imaging (a) the core, with a higher density is brighter, while in bright field (b) the core is darker. The average core radius in samples grown with lower CO concentration is inferior.

A change in the precursor concentration seems to have minor effect on the wires diameter. The variation of core and shell diameters is summarized in Figure 9.

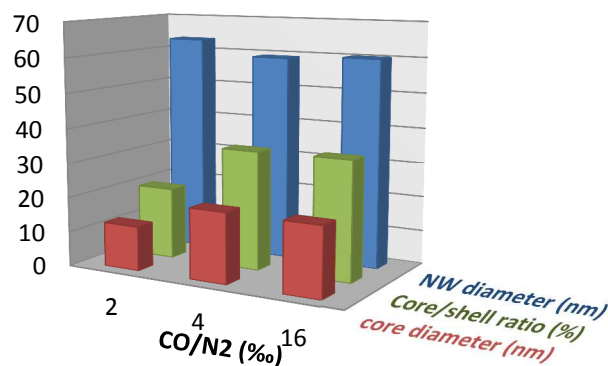


**Figure 9:** variation of core and shell diameter versus precursor concentration (in logarithmic scale)

## Conclusions

Using a simple thermal CVD system it was possible to synthesize core/shell SiC/SiO<sub>2</sub> nanowires on silicon substrates using gaseous precursor (CO).

It was demonstrated that using a commercial surfactant it was possible to obtain a uniform catalyst layer on silicon substrate and consequently a homogeneous growth.

Varying growth parameters it was found a way to control SiC core presence and diameter inside the wires. It was found that wires' core diameter is proportional to precursor concentration during the synthesis, in addition there is a direct influence of growth temperature over the formation of the SiC core.

## Acknowledgements

The research is partly supported by the FP7 MARIE CURIE ITN Project "Nanowiring" and by the Project "BioNiMed" funded by the bank foundation Fondazione Cariparma.

## Notes and references

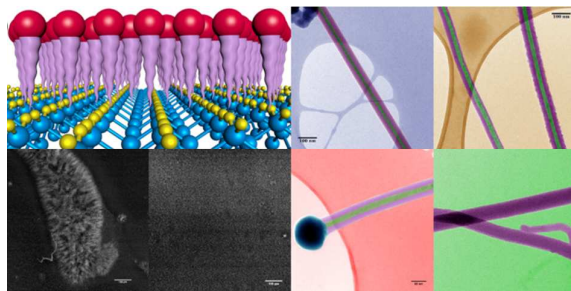
<sup>a</sup> University of Parma, via Università 12 - 43121 Parma (Italy).

<sup>b</sup> IMEM-CNR, Parco Area delle Scienze 37A, 43124 Parma (Italy)

† Electronic Supplementary Information (ESI) available: Experimental details of the sample preparation. SEM images of core-shell nanowires samples prepared with and without surfactant. STEM-HAADF of a single core-shell nanowire. See DOI: 10.1039/b000000x/

1. Y. Xia, P. Yang, Y. Sun, Y. Wu, B. Mayers, B. Gates, Y. Yin, F. Kim, and H. Yan, *Adv. Mater.*, 2003, **15**, 353–389.
2. G. Attolini, F. Rossi, F. Fabbri, G. Salviati, M. Bosi, and B. E. Watts, *Mater. Sci. Forum*, 2012, **711**, 75–79.
3. W. J. Choyke, H. Matsunami, and G. Pensl, *Silicon Carbide: Recent Major Advances*, Springer, 2004.
4. R. Yakimova, R. M. Petoral, G. R. Yazdi, C. Vahlberg, A. Lloyd Spetz, and K. Uvdal, *J. Phys. D: Appl. Phys.*, 2007, **40**, 6435–6442.
5. S. E. Saddow, *Silicon Carbide Biotechnology: A Biocompatible Semiconductor for Advanced Biomedical Devices and Applications*, Elsevier, Waltham, MA, 2012.
6. S. E. Saddow and A. Agarwal, *Advances in Silicon Carbide Processing and Applications*, Artech House, 2004.
7. G. Attolini, F. Rossi, M. Bosi, B. E. Watts, and G. Salviati, *J. Non. Cryst. Solids*, 2008, 5227–5229.
8. W.-S. Seo, K. Koumoto, and S. Aria, *J. Am. Ceram. Soc.*, 2004, **83**, 2584–2592.
9. W. Yang, H. Miao, Z. Xie, L. Zhang, and L. An, *Chem. Phys. Lett.*, 2004, **383**, 441–444.
10. S. G. Sundaresan, A. V. Davydov, M. D. Vaudin, I. Levin, J. E. Maslar, Y.-L. Tian, and M. V. Rao, *Chem. Mater.*, 2007, **19**, 5531–5537.
11. W. Shi, Y. Zheng, H. Peng, N. Wang, C. S. Lee, and S.-T. Lee, *J. Am. Ceram. Soc.*, 2000, **83**, 3228–3230.
12. T. Seeger, P. Kohler-Redlich, and M. Rühle, *Adv. Mater.*, 2000, **12**, 279–282.
13. G. Yang, R. Wu, J. Chen, Y. Pan, R. Zhai, L. Wu, and J. Lin, *Nanotechnology*, 2007, **18**, 155601.
14. H. Dai, E. W. Wong, Y. Z. Lu, S. Fan, and C. M. Lieber, *Nature*, 1995, **375**, 769–772.
15. E. W. Wong, *Science (80-. )*, 1997, **277**, 1971–1975.
16. F. Patolsky, G. Zheng, and C. M. Lieber, *Anal. Chem.*, 2006, **78**, 4260–4269.
17. F. Fabbri, F. Rossi, G. Attolini, G. Salviati, S. Iannotta, L. Aversa, R. Verucchi, M. Nardi, N. Fukata, B. Dierre, and T. Sekiguchi, *Nanotechnology*, 2010, **21**, 345702.

18. F. Fabbri, F. Rossi, G. Attolini, G. Salviati, B. Dierre, T. Sekiguchi, and N. Fukata, *Mater. Lett.*, 2012, **71**, 137–140.
19. E. Denkhaus and K. Salnikow, *Crit. Rev. Oncol. Hematol.*, 2002, **42**, 35–56.
20. B. Park, Y. Ryu, and K. Yong, *Surf. Rev. Lett.*, 2004, **11**, 373–378.
21. G. A. Swift and R. Koc, *J. Mater. Sci.*, 2001, **36**, 803–806.
22. X. G. Zhang, *Electrochemistry of Silicon and Its Oxide*, Springer, 2001.
23. H. Ubara, T. Imura, and A. Hiraki, *Solid State Commun.*, 1984, **50**, 673–675.
24. T. Young, *Philos. Trans. R. Soc. London*, 1805, **95**, 65–87.
25. N. A. Ivanova and V. M. Starov, *Curr. Opin. Colloid Interface Sci.*, 2011, **16**, 285–291.
26. M. A. A. Elmasry, A. Gaber, and E. M. H. Khater, *J. Therm. Anal. Calorim.*, 1998, **52**, 489–495.
27. R. S. Wagner and W. C. Ellis, *Appl. Phys. Lett.*, 1964, **4**, 89.
28. F. Fabbri, F. Rossi, M. Negri, R. Tatti, L. Aversa, S. Chander Dhanabalan, R. Verucchi, G. Attolini, and G. Salviati, *Nanotechnology*, 2014, **25**, 185704.

**Table of contents**

Varying the growth conditions in chemical vapour deposition synthesis we demonstrate the possible tuning of the core-shell ratio of SiC/SiO<sub>2</sub> nanowires